The effect of compaction and shear deformation of saturated soil on hydraulic conductivity

Published version:

DOI:DOI: 10.1016/j.still.2012.05.020

Soil & Tillage Research 125 (2012) 23–29

Contents lists available at SciVerse ScienceDirect

Soil & Tillage Research

journal homepage: www.elsevier.com/locate/still

The effect of compaction and shear deformation of saturated soil on hydraulic conductivity

W.R. Whalley [a,*], G.P. Matthews [b], S. Ferraris [c]

[a] Rothamsted Research, Harpenden, Hertfordshire AL5 2JQ, UK
[b] Environmental and Fluid Modelling Group, University of Plymouth, Plymouth, Devon PL4 8AA, UK
[c] Interuniversity Department of Regional and Urban Studies and Planning, Università degli Studi di Torino e Politecnico di Torino, viale Mattioli 39, Torino 10125, Italy

ARTICLE INFO

Keywords:
Consolidation
Critical state
Clay soil
Empirical models

ABSTRACT

This paper describes how in a clay soil, consolidation and then shear deformation at a constant porosity affect the hydraulic conductivity of the saturated soil. We used a Bishop and Wesley triaxial cell to consolidate the soil along the normal consolidation line and then to shear-deform the soil at a constant porosity to the point where the critical state condition had been reached. The relationship between hydraulic conductivity (k_{sat}) and soil porosity for soil consolidated on the normal consolidation line was similar to previously published data. However, shear deformation of soil when held at a constant porosity greatly reduced k_{sat} especially at high porosity, where k_{sat} was reduced to 5% of its original value. In dense soil the effects of shear deformation on k_{sat} were smaller. We used previously published water release data for the variously compacted and shear deformed soil to estimate water release curves for the soil in our experiment. We showed that an empirical model to predict k_{sat} gave a good fit to our experimental data collected in the laboratory. We tested the empirical model on a wider set of field data obtained from the HYPRES data base.

1. Introduction

When soil is damaged in the field, because of traffic by agricultural machinery, it is often referred to as "compacted". However, in practice in the top soil, so-called compaction events are usually a combination of densification and shear deformation. Green et al. (2003) have reviewed the effects of various types of soil deformation on hydraulic conductivity. Their conclusion, in agreement with many other studies (Matthews et al., 2010; Reynolds et al., 2008; Wang and Huang, 1984), is that saturated hydraulic conductivity is very sensitive to changes in porosity. Many of the effects of soil type and compaction can be taken into account with the use of an effective porosity. Carman (1939) was one of the first to propose this approach to allow the saturated hydraulic conductivity k_{sat} in clays and sands to be described by a single equation. The Kozeny–Carman (KC) equation is widely used to explore the effects of changes in porosity on hydraulic conductivity. It is written as:

$$k_{sat} = \tau \frac{1}{S^2} \frac{\rho_w^2 g}{\nu \rho_s^2} \frac{e^3}{1+e} \qquad (1)$$

where S is the specific surface area, τ is a tortuosity factor, g is the acceleration due to gravity, ρ_w and ρ_s are the density of water and soil respectively, ν is the dynamic viscosity of water and e is the void ratio (note: $e = \phi/(1-\phi)$, where ϕ is porosity) (see Chapuis and Aubertin, 2003). However, Chapuis and Aubertin (2003) observed that the KC equation is rarely used because of the difficulty of measuring the parameters, especially S. An additional complication is that τ is a constant that takes account of differences in tortuosity between different soils, and if k_{sat} is to be predicted τ needs to be known. However, Carman (1939) expected that τ would only have a narrow range of values.

The relationship between soil porosity and hydraulic conductivity is often described by an empirical power law (Ahuja et al., 1989; Aminrun et al., 2004; Green et al., 2003):

$$k_{sat} = B\phi_e^n \qquad (2)$$

where B and n are fitted, and ϕ_e is the effective porosity which is defined as the difference between the water content at saturation θ_s and at a more negative matric potential. There is a general view that Eq. (2) is a Kozeny–Carmen derived relationship, although the resemblance is not very strong as far as the form of the equation is concerned. In fact the functional relationship is different to the one described by Carman (1939). Typically n is assumed have a value between 4 and 5, and B may vary with soil type (Ahuja et al., 1989). The approach recognises that the hydraulic conductivity of saturated soil depends mainly on the larger voids (i.e. those affecting the saturated end of the water retention curve). The choice of the lower value of matric potential, used to estimate ϕ_e, is

* Corresponding author.
E-mail address: richard.whalley@rothamsted.ac.uk (W.R. Whalley).

0167-1987/$ – see front matter © 2012 Elsevier B.V. All rights reserved.
http://dx.doi.org/10.1016/j.still.2012.05.020

arbitrary. Ahuja et al. (1989) recommend −33 kPa whereas Aminrun et al. (2004) suggest that a more negative value of −66 kPa may work better for soil with higher clay content. Han et al. (2008) estimated ϕ_e from the point of inflexion of the water retention curve, which was determined from a fit of the Van Genuchten function (van Genuchten, 1980). With this general approach, it does seem possible to obtain an approximately common relationship between k_{sat} and ϕ_e for different soils as well as describe the effects of soil damage by compaction on k_{sat} (Green et al., 2003). However, individual soil types have systematic variations from the average curve fitted to a number of soils (see Fig. 4a in Ahuja et al., 1989). Assouline and Or (2008) outline how, in addition to porosity, the air entry potential can be used in an improved approach to take account of the effects of compaction on hydraulic conductivity.

Matthews et al. (2010) have proposed a simple model for saturated hydraulic conductivity using the water retention characteristic. They considered the interconnection of cylinders of different sizes across a section of a porous material. In a special case it was assumed that these interconnections were random. A distribution $F(r)$ of cylindrical pore radii r was derived from the water retention curve (θ, ψ) as:

$$F(r) = \frac{d\theta}{dr} = \frac{d\psi}{dr}\frac{d\theta}{d\psi} \tag{3}$$

where ψ is the matric potential. Assuming that the flow of water through a cylinder was proportional to its cross-sectional area, then,

$$k_{sat} \propto [\int_0^1 rF(r)dr]^2 \tag{4}$$

Commonly this expression is incorporated into a model for relative permeability or unsaturated hydraulic conductivity, appearing as a denominator in such a model (Mualem, 1976).

A constant of proportionality is required to achieve absolute values of k_{sat} from Eq. (4) which may be written as:

$$k_{sat} \propto \left[\int_0^1 \frac{1}{\psi} d\theta\right]^2 \tag{5}$$

Matthews et al. (2010) used the van Genuchten function for the water retention characteristic (van Genuchten, 1980) to evaluate this integral and used the standard constraint $m = 1-1/n$ for the two shape parameters of the water retention characteristic.

With the change of variable

$$\Theta = \frac{\theta - \theta_r}{\theta_s - \theta_r} \tag{6}$$

where θ_s and θ_r are the respective saturated and residual water contents, Eq. (5) became:

$$k_{sat} \propto (\theta_s - \theta_r)^2 \left[\int_0^1 \frac{1}{\psi} d\Theta\right]^2 \tag{7}$$

which was rewritten as:

$$k_{sat} \propto \alpha^2(\theta_s - \theta_r)^2 \left[\int_0^1 \left(\frac{\Theta^{1/m}}{1-\Theta^{1/m}}\right)^{1-m} d\Theta\right]^2 \tag{8}$$

where α was the third fitting parameter for the Van Genuchten function.

The integral in Eq. (8) equates to 1 and it can be written as:

$$k_{sat} \propto \alpha^2(\theta_s - \theta_r)^2 \tag{9}$$

A constant of proportionality needed to achieve absolute values may be inserted in Eq. (9) to give:

$$k_{sat} = \frac{\rho_w g}{8\upsilon}\left(\frac{2\gamma}{\rho_w g}\right)^2 \alpha^2(\theta_s - \theta_r)^2 \tag{10}$$

where υ is the viscosity of water and γ is the surface tension of water. Here we assume no requirement for a correction factor to account for tortuosity. Eq. (10) simplifies to:

$$k_{sat} = \frac{\gamma^2}{2\upsilon\rho_w g}\alpha^2(\theta_s - \theta_r)^2 \tag{11}$$

Matthews et al. (2010) explored the effects of isotropic compression on the hydraulic conductivity of soil. They found that both Eq. (11) and a pore network model gave good predictions of the effects of consolidation on the change in hydraulic conductivity, although the absolute predicted values were in some error.

Soil deformations can be more complex than merely an increase in soil density and may include the effects of shear deformation. The critical state description of soil behaviour allows the relationships between compression, shear deformation and soil porosity to be defined. During critical state deformation the soil is completely destructured (Mitchell and Soga, 2005) to the extent that there is no evidence of any aggregation and the entire pore space can be assumed to be textural. At the critical state, the shear stress and density remain constant while shear strain increases. Depending on the initial state of the soil, its porosity will either increase or decrease as it is shear deformed to approach the critical state. Kirby and Blunden (1991) considered the effect of both of these transitions to the critical state on soil hydraulic properties.

In newly cultivated soils it is likely that porosity will decrease during shear. We were interested to discover if relationships between soil porosity and its hydraulic conductivity for saturated soil were different for normally consolidated soil compared with soil which had been shear deformed. Although the effects of a change in porosity on hydraulic conductivity are widely reported, there are very little published data on the effect of shear deformation on soil hydraulic conductivity (Kirby and Blunden, 1991).

2. Materials and methods

2.1. Soil sample and preparation

We used Rowden soil (Gregory et al., 2010a, b; Matthews et al., 2010) which is a clay soil from North Wyke, Devon, UK. Basic soil

Table 1
Basic soil properties.

Location		North Wyke, Devon
Field		Rowden
Grid reference	GB National Grid	SX652994
	Longitude	03,54,50 W
Soil type	Latitude	50,46,43 N
	SSEW group	Stagnogley soil
	SSEW series	Hallsworth
	FAO	Gleyic Luvisol
Land use		Permanent grass
Sand 2000–63 μm	$g\,g^{-1}$ dry soil	0.147
Silt 63–2 μm	$g\,g^{-1}$ dry soil	0.396
Clay < 2 μm	$g\,g^{-1}$ dry soil	0.457
Texture	SSEW	Clay
Particle density	$g\,cm^{-3}$	2.466
Organic matter	$g\,g^{-1}$ dry soil	0.076

properties were measured by standard methods (Table 1). The air dried soil was crumbled to pass a 4 mm sieve and left to air-dry in a single bulked sample. Before use the soil was equilibrated to a water content of 0.55 g g^{-1} by adding water and storing in a fridge. The soil was packed into a mould 38 mm in diameter and 78 mm long in thin layers, approximately 1 cm deep. Each layer was compressed uniaxially with a pneumatic press at a pressure of 10 kPa.

2.2. Measuring k_{sat} in consolidation and shear deformed soil

We used a Bishop and Wesley triaxial cell (Ng and Menzies, 2007) to deform the soil and measure hydraulic conductivity (see Fig. 1). Once in the triaxial cell, the soils were saturated by increasing the pressure of the water confining the soil sample and the pressure of the soil water to 600 and 590 kPa respectively over a period of 24 h. The soils were then consolidated to a range of effective stresses between 10 (initial condition) and approximately 500 kPa. Isotropic compression was achieved by adjusting the relative values of the pore pressure and cell pressure to increase the effective stress on the saturated soil sample. The normal consolidation line was determined from a number of independent consolidation tests. Following consolidation of samples, shear deformation was applied by raising the pedestal (see Fig. 1). During shear deformation, the volume of the sample was kept constant by fixing the volume of the pore-pressure pressure volume controller and the change in the pore pressure was monitored (see Fig. 1). During shear deformation, the soil sample shape changed from cylindrical (at the end of normal consolidation) to barrel-shaped (at the end of shear deformation).

The triaxial cell we used had an additional pressure volume controller connected to the base of the sample, so we were able to measure the flux of water through a sample at any given hydraulic gradient. We applied a hydraulic gradient of 20 kPa across the sample as described by Matthews et al. (2010). The hydraulic conductivity of the cylindrical samples was readily calculated.

To convert the flux of water measured through the barrel-shaped shear-deformed samples into a hydraulic conductivity we assumed that the soil had the diameter of a cylinder with the volume of the barrel and with the same height. To determine the magnitude of any error arising from the assumption of an equivalent volume cylinder, the Darcy equation was integrated in an axial symmetrical domain by a finite volume code (Manzini and Ferraris, 2004) for two geometries; a barrel shaped sample and a cylinder of the same height with an equivalent volume diameter. For a given value of k_{sat} (1.14 cm/s) and hydraulic gradient (20 kPa)

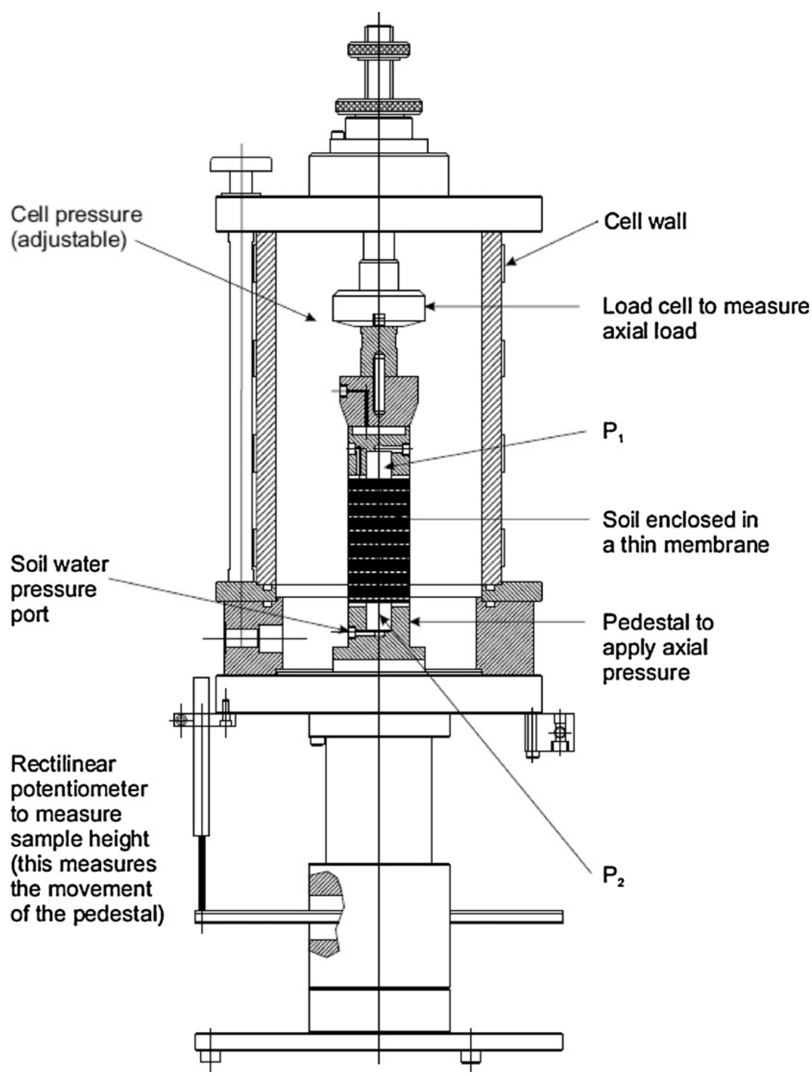

Fig. 1. Bishop and Wesley cell used to consolidate and shear the soil and then to measure the saturated hydraulic conductivity of soil. A hydraulic gradient can be applied by adjusting the pressure of the water at the top of the sample P_1 relative to the pressure of the water at the base of the sample P_2.
Redrawn from Whalley et al. (2011) and a diagram originally supplied by Jerry Sutton (GDS Instruments, 32 Murrel Green Business Park, Hook, Hampshire, RG UK).

the modelled fluxes from these two geometries were similar ($30.4\ cm^3/h$ for the barrel compared to $34.1\ cm^3/h$ for the equivalent diameter cylinder).

2.3. Use of published data

Empirical models to predict k_{sat} usually require the water retention characteristic to be known to some extent. To estimate the water retention characteristic curves of the deformed soils in this paper we used the data published by Gregory et al. (2010a). They reported water release characteristic data for Rowden soil which was compressed uniaxially and also soil shear deformed, by remoulding, which was fitted to the following:

$$\theta = \left[\frac{\theta_s - \theta_r}{(1 + (\phi^b \psi)^{nv})^{1-(1/nv)}} \right] + \theta_r \qquad (12)$$

where ϕ is the soil porosity and b is a parameter that depends on soil damage. Parameters θ_s, θ_r, α (here $\alpha = \phi^b$) and n_v are those of the van Genuchten function. The value of b increases with soil damage. We assumed that remoulding of soil by Gregory et al. (2010a, b) had the same effects as soil deformation at the critical state and hence that the values of b for remoulded soil applied to soil at the critical state.

To test empirical models for k_{sat} more widely we used hydraulic conductivity data for saturated from the HYPRES data base along with estimates of the Van Genuchten parameters for the same soils. The most comprehensive ('L') dataset of the HYPRES database (Wösten et al., 1999) was used. The extracted data were restricted to topsoils (not all were cultivated) and subsoils, to depths of 2.3 m. Buried, organic or ambiguous horizons were omitted.

3. Results and discussion

3.1. Soil deformation

The normal consolidation curve is shown in Fig. 2A. This is consistent with data published for the same soil by Matthews et al. (2010). The critical state line is also shown in Fig. 2A and it is consistent with previously published data for clay soils (O'Sullivan and Robertson, 1996) in that its slope is slightly steeper than that of the normal consolidation line. In Fig. 2B the deviator stress is plotted against the mean stress. The deviator stress varies linearly with the mean stress. In all cases shear deformation resulted in visible barrelling of an initially cylindrical soil sample (see Mitchell and Soga, 2005).

3.2. Deformation and hydraulic conductivity

The hydraulic conductivity of soil is plotted against porosity in Fig. 3. For normally consolidated soil the data are typical of widely reported correlations between consolidation and hydraulic conductivity (e.g. Matthews et al., 2010). When the soil was shear deformed to the critical state, k_{sat} was smaller for any given porosity compared to its initial value when the soil was normally consolidated (see Fig. 3). We fitted

$$\log_{10} k_{sat} = R\phi + Q \qquad (13)$$

to the data in Fig. 3 where ϕ is porosity. The values of the parameters, R and Q are given in Table 2, together with the standard errors (SE). The fitted curves explained 90 percent of the variance ($P < 0.002$) in k_{sat} for the normally consolidated soil and 85 percent of the variance ($P < 0.005$) in k_{sat} for soil at the critical state.

In this clay soil at a porosity of 62 percent, shear deformation reduced k_{sat} to 5 percent of its original value. In the most compacted soil the effect of shear deformation on k_{sat} was smaller. If the fitted lines in Fig. 3 are extrapolated to lower porosities, they meet at 56 percent. Therefore, if soil at a porosity of around 56%, was shear deformed, the effect on k_{sat} is likely to be very small.

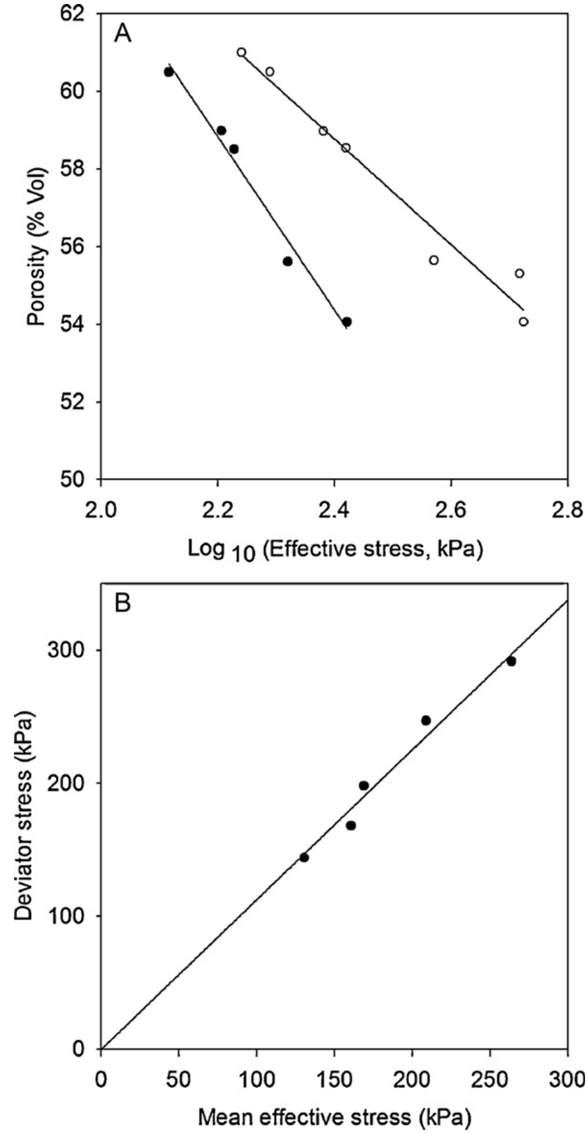

Fig. 2. (A) Porosity as a function of the logarithm of mean effective stress for soil which is either normally consolidated (open symbols) or in the critical state condition (closed symbols). (B) Deviator stress plotted against the mean stress for soil which has been shear deformed to the extent that it is in the critical state condition.

Table 2
Fitted values of R and Q in Eq. (13) and their standard errors.

Soil condition	Parameter				Percentage of variance accounted for and P value
	R	SE	Q	SE	
Normally consolidated	0.4836	0.0683	−29.35	4.20	90.8, $P < 0.002$
Critical state	0.3024	0.0547	−19.22	3.36	85.5, $P < 0.005$

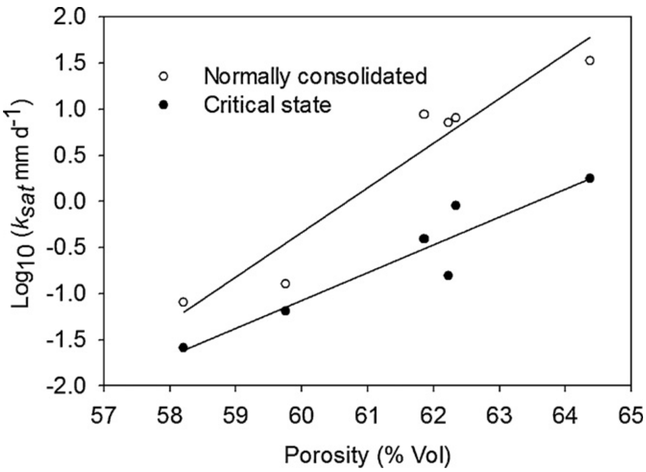

Fig. 3. The logarithm of hydraulic conductivity for normally consolidated soil (open symbols) and for soil in the critical state (closed symbols) plotted against porosity. The data are fitted to Eq. (13) and the fitted parameters are given in Table 2.

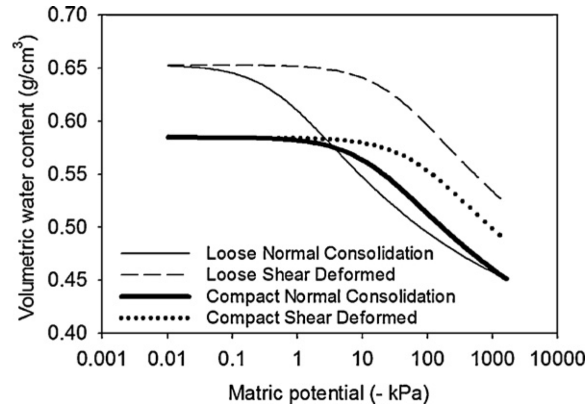

Fig. 4. Estimated water release curves for normally consolidated loose and compact soil as well as shear deformed loose and compact soil. These curves were estimated using parameters of Eq. (12) in Table 3 for variously compacted and shear deformed Rowden soil published by Gregory et al (2010).

3.3. *Empirical predictions of* k_{sat} *based on the water release characteristic: laboratory data*

Most empirical methods used to predict hydraulic conductivity, including Eqs. (2) and (9), require some information from the water release characteristic. We used published data for variously damaged Rowden soil (Gregory et al., 2010a) which are listed in Table 3 to estimate water release characteristics with Eq. (12) (see Fig. 4). These estimated water release characteristics were used to estimate ϕ_e and $\alpha(\theta_s - \theta_r)$ of the loose soil, dense soil, shear deformed loose soil and shear deformed dense soil (see Table 3). The effective porosities were determined from the difference between the saturated water contents and the water contents at a matric potential of −33 kPa (see Table 3).

The values of k_{sat} corresponding to those porosities of soils for which water release data were available were determined with Eq. (13) and *R* and *Q* values given in Table 2. The fitted values of the exponent and constant in Eqs. (2) and (9) are given in Table 4 (see Fig. 5). The value of the exponent in Eq. (2) was 4.04, similar to those previously reported (Ahuja et al., 1989; Green et al., 2003), although Mavko and Nur (1997) observed that the *n* exponent in Eq. (2) is an *ad hoc* solution to the problem of empirically reducing k_{sat} with porosity and that *n* varies from 3 to 8 depending on soil. The fitted exponent in Eq. (9) was 1.651 and it was not statistically significantly different to the expected value of 2 (Table 4 and Fig. 5B).

3.4. *Empirical predictions of* k_{sat} *based on the water release characteristic: field data*

We explored the possibility for the more general use of Eq. (9) using data from a wider range of soils from the HYPRES data base. In Fig. 6 the fitted k_{sat} data are plotted against the measured values with the relationship:

$$\log_{10}k_{sat} = 2\log_{10}(\alpha(\theta_s - \theta_r)) + 4.119. \quad (14)$$

We kept the exponent at its theoretical value of 2 and only adjusted the linear constant during the fitting process.

The laboratory data collected in this study and field data from HYPRES did not seem to be in good agreement. Fig. 6 shows that Eq. (14) overestimated the saturated hydraulic conductivities measured in this work by up to 2½ orders of magnitude, although the errors were within the scatter of the HYPRES data. However, Eq. (14) correctly predicted the trend in the measured data. The differences could be attributed to the fact that our soils were

Table 3
Parameters derived from the estimated water release characteristics shown in Fig. 4 along with the k_{sat} data calculated from the appropriate porosity, i.e. θ_s the saturated water content with Eq. (12).

Soil condition	Effective porosity	$\theta_s - \theta_r$	b	θ_s	n_v	α i.e. ϕ^b	$\alpha\ (\theta_s - \theta_r)$	k_{sat} (mm day^{-1} calculated with Eq. (12) for appropriate porosity θ_s)
Loose	0.135	0.451	−1.25	0.650	1.187	1.713	0.7727	121.388
Loose and shear deformed	0.030	0.205	6.72	0.650	1.187	0.0554	0.0114	0.0624
Compact	0.045	0.303	4.04	0.582	1.187	0.1123	0.0339	2.7289
Compact and shear deformed	0.014	0.138	6.71	0.582	1.187	0.0264	0.0036	0.0239

Table 4
Values of the parameters fitted to Eqs. (2) and (9) using the data in Fig. 5.

Equation	Units of K_s	Units of specified parameter	Fitting parameter	Value of fitting parameter	Percentage of variance accounted for and *P* value
$k_{sat} = B\phi_e^n$	mm day^{-1}		B	348,096	89.5%, $P = 0.036$
			n	4.04	
$k_{sat} = C\alpha^v(\theta_s - \theta_r)^v$	mm day^{-1}	α (kPa^{-1})	C	243	97.5%, $P = 0.023$
			v	1.651[a]	

[a] This exponent is written as 2 in Eq. (9). Here the fitted value is given.

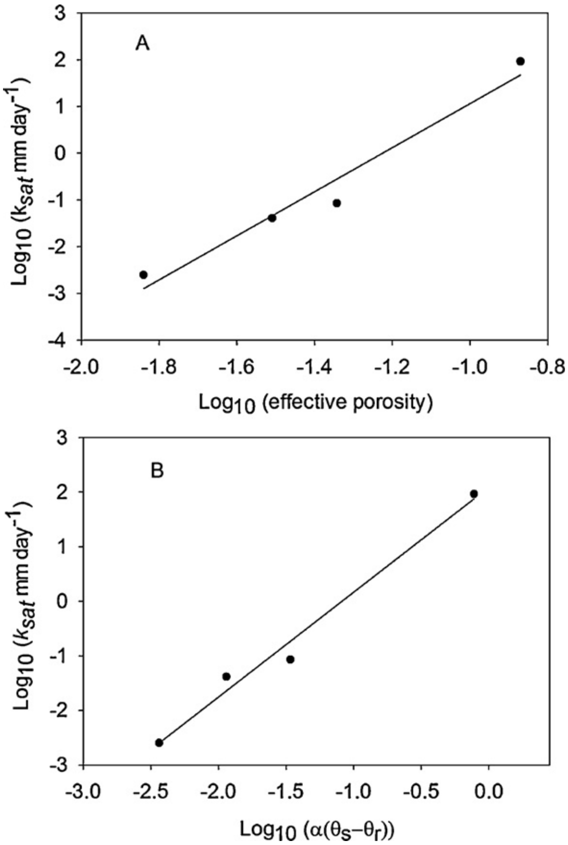

Fig. 5. The logarithm of hydraulic conductivity k_{sat} plotted against the logarithm of effective porosity (panel A) and the logarithm of $\alpha(\theta_s - \theta_r)$ (panel B). Both the effective porosity and $\alpha(\theta_s - \theta_r)$ were determined form the water release characteristics shown in Fig. 4 (see Table 3). The fitted parameters of Eq. (2) for the top panel and Eq. (9) for the bottom panel are given in Table 4.

repacked whereas the soils used to generate the HYPRES database were undisturbed, or that we used estimated and not measured water release data (Fig. 4). Nevertheless it is clear that Eq. (14), with only one arbitrary fitting parameter and other parameters obtainable from the water retention characteristic, provides a useful fit to the HYPRES data and the experimental data obtained from repacked soil.

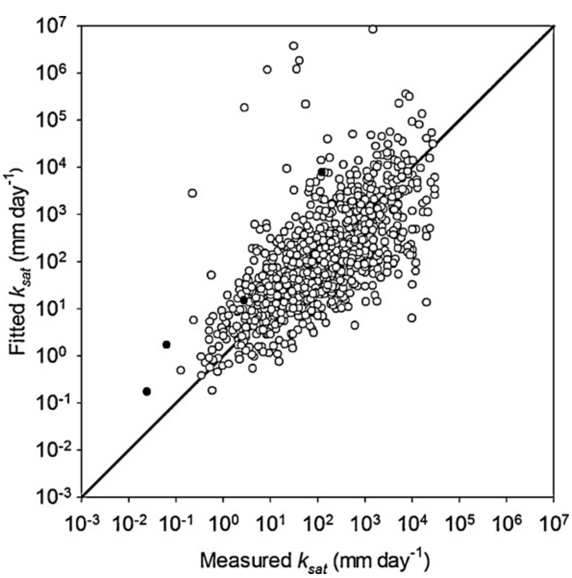

Fig. 6. Fitted k_{sat} plotted against measured k_{sat} (on a log scale). Open circles are data from the HYPRES database. Fitted data were obtained from Eq. (14). Also plotted are the data predicted with Eq. (14) for the compacted and sheared soil samples in this study (closed circles) using the fitting parameter obtained from the HYPRES data.

3.5. The implications of our findings

Our data implies that soil macrostructure in loose soil is very sensitive to damage by shear deformation. In the field, isotropic consolidation is likely to be a rare occurrence. Uniaxial compression is often used in the laboratory to replicate the effects of compaction (Gregory et al., 2006), but this is a combination of consolidation and shear deformation and will probably result in a k_{sat} for any given porosity that is between the limits of those values for "normal consolidation" and the "critical state" shown in Fig. 3.

The two empirical models for k_{sat} appeared to be effective at describing the effects of complex deformations on k_{sat}. However, the requirement for prior knowledge of the water release characteristic makes these empirical approaches difficult to use in practice. Nevertheless, we have shown that there is scope to use relatively simple empirical approaches to describe the effect of soil deformation on the water release characteristic which can then be used to explain how k_{sat} varies with soil deformation. The effective porosity approach (Eq. (2)) required the water content at saturation and one other more negative matric potential. The use of Eq. (9) was further complicated because the value of α also needed to be known or estimated. When water release data were available, a relatively simple model for k_{sat} (Eqs. (9) and (14)) appeared to be useful over a wide range of soils which had been variously damaged.

4. Conclusions

Shear deformation of loose soil at a constant porosity can result in a large reduction in the saturated hydraulic conductivity k_{sat}. Reductions in k_{sat} following compaction and/or shear deformation are predictable if the effect of soil deformation on the water release characteristic is either known or can be estimated. We have tested an empirical equation to estimate k_{sat} using the HYPRES database, and established its utility for predicting k_{sat} in the field.

Acknowledgements

This work was funded by a grant from the UK Engineering and Physical Sciences Research Council (EPSRC) (EP/H040064/1) and Italian Government grant PRIN2007 "Experimental measurement of the soil-vegetation-atmosphere interaction processes and numerical modelling of their response to climate change". The facilities at Rothamsted Research were funded by the UK Biotechnology and Biological Sciences Research Council (BBSRC). We are indebted to Allan Lilly of the James Hutton Institute, Aberdeen who extracted hydraulic data of soil from the HYPRES data base on 27th July 2011.

References

Ahuja, L.R., Cassel, D.K., Bruce, R.R., Barns, B.B., 1989. Evaluation of spatial distribution of hydraulic conductivity using effective porosity data. Soil Science 148, 404–411.

Aminrun, W., Amin, Ms.M., Eltaib, S.M., 2004. Effective porosity of paddy soils as an estimate of its saturated hydraulic conductivity. Geoderma 121, 197–203.

Assouline, S., Or, D., 2008. Air entry-based characteristic length for estimation of permeability of variably compacted earth materials. Water Resources Research 44, W11403, http://dx.doi.org/10.1029/2008WR006937.

Carman, P.C., 1939. Permeability of sands soils and clays. Journal of Agricultural Science 29, 262–273.

Chapuis, R.P., Aubertin, M., 2003. On the use on the Kozeny–Carman equation to predict the hydraulic conductivity of soils. Canadian Geotechical Journal 40 616-613.

Green, T.R., Ahuja, L.R., Benjamin, J.G., 2003. Advances in predicting agricultural management effects on soil hydraulic properties. Geoderma 116, 3–27.

Gregory, A.S., Whalley, W.R., Watts, C.W., Bird, N.R.A., Hallett, P.D., Whitmore, A.P., 2006. Calculation of the compression index and the precompression stress from soil compression test data. Soil and Tillage Research 89, 45–57.

Gregory, A.S., Bird, N.R.A., Whalley, W.R., Matthews, G.P., Young, I.M., 2010a. Deformation and shrinkage effects on the soil water release characteristic. Soil Science Society of America Journal 74, 1104–1112.

Gregory, A.S., Bird, N.R.A., Whalley, W.R., Matthews, G.P., 2010b. Estimating relative hydraulic conductivity from the water release characteristic of a shrinking clay soil. Soil Science Society of America Journal 74 1113-1113.

van Genuchten, M.T., 1980. A closed-form equation for predicting the hydraulic conductivity of unsaturated soils. Soil Science Society of America Journal 44, 892–898.

Han, H., Gimenez, D., Lilly, A., 2008. Textural averages of saturated soil hydraulic conductivity predicted from water retention data. Geoderma 146, 121–128.

Kirby, J.M., Blunden, B.G., 1991. Interaction of soil deformations, structure and permeability. Australian Journal of Soil Research 29, 891–904.

Mavko, G., Nur, A., 1997. The effect of a percolation threshold in the Kozeny–Carman relation. GeoPhysics 62, 1480–1482.

Manzini, G., Ferraris, S., 2004. Mass-conservative finite-volume methods on 2-D unstructured grids for the Richards equation. Advances in Water Resources 27, 1199–1215.

Matthews, G.P., Laudone, G.M., Gregory, A.S., Bird, N.R.A., Matthews, A.G.D.G., Whalley, W.R., 2010. Measurement and simulation of the effect of compaction on the pore structure and saturated hydraulic conductivity of grassland and arable soil. Water Resources Research 46, W05501, http://dx.doi.org/10.1029/2009WR007720.

Mitchell, J.K., Soga, K., 2005. Fundamentals of Soil Behaviour. Wiley & Sons, NJ, USA, 577 p.

Mualem, Y., 1976. A new model for the predicting the hydraulic conductivity of unsaturated porous media. Water Resources Research 12 (3), 513–522 1976.

Ng, C.W.W., Menzies, B., 2007. Advanced Unsaturated Soil Mechanics and Engineering. Taylor and Francis, Abingdon, Oxfordshire, UK.

O'Sullivan, M.F., Robertson, E.A.G., 1996. Critical state parameters from intact samples of two agricultural top soils. Soil and Tillage Research 39, 161–173.

Reynolds, W.D., Durury, C.F., Yang, X.M., Tan, C.S., 2008. Optimal soil physical quality inferred through structural regression and parameter interaction. Geoderma 146, 466–474.

Wang, M.C., Huang, C.C., 1984. Soil compaction and permeability prediction models. ASCE Journal of Environmental Engineering 110, 1063–1083.

Whalley, W.R., Jenkins, M., Attenborough, K., 2011. The velocity of shear waves in saturated soil. Soil Science Society of America Journal 75, 1652–1657.

Wösten, J.H.M., Lilly, A., Nemes, A., Le Bas, C., 1999. Development and use of a database of hydraulic properties of European soils. Geoderma 90, 169–185.